Editors' Suggestion

Vibronic Coupling through the Continuum in the $e + CO_2$ System

Jan Dvořák,[1] Miloš Ranković,[2] Karel Houfek,[1] Pamir Nag,[2] Roman Čurík,[2] Juraj Fedor,[2,*] and Martin Čížek[1,†]

[1]Charles University, Faculty of Mathematics and Physics, Institute of Theoretical Physics, V Holešovičkách 2, 180 00 Prague 8, Czech Republic

[2]J. Heyrovský Institute of Physical Chemistry, Czech Academy of Sciences, Dolejškova 2155/3, 182 23 Prague 8, Czech Republic

(Received 11 February 2022; revised 20 April 2022; accepted 20 May 2022; published 27 June 2022)

We report two-dimensional electron energy-loss spectra of CO_2. The high-resolution experiment reveals a counterintuitive fine structure at energy losses where CO_2 states form a vibrational pseudocontinuum. Guided by the symmetry of the system, we constructed a four-dimensional nonlocal model for the vibronic dynamics involving two shape resonances (forming a Renner-Teller Π_u doublet at the equilibrium geometry) coupled to a virtual Σ_g^+ state. The model elucidates the extremely non-Born-Oppenheimer dynamics of the coupled nuclear motion and explains the origin of the observed structures. It is a prototype of the vibronic coupling of metastable states in continuum.

DOI: 10.1103/PhysRevLett.129.013401

The most striking phenomena in the electron-molecule scattering are often related to the formation of compound anionic states [1,2]. These states can have a mixed character combining bound states with resonances or virtual states [3]. The vibrational dynamics of such states can be represented by the familiar motion of nuclei on a potential energy surface (PES). The resonant PESs have, however, an imaginary component due to the embedding in the continuum and become nonlocal and energy dependent in the full form. This approach is well established for the theoretical treatment of the electron scattering from diatomic molecules including the understanding of the importance of the nonlocality for reproduction of many features observed in the cross sections [2,3]. In polyatomic molecules a local complex potential approximation has almost exclusively been applied [4–7]. The intersection of multiple electronic states in the continuum has a specific topology due to the presence of the imaginary part [8–11]. Unlike in the case of bound states [12], the vibronic interaction of short-lived states is relatively unexplored. Estrada *et al.* [13] performed a full nonlocal dynamical calculation for a model system with two vibrational degrees of freedom and two states vibronically coupled (pseudo-Jahn-Teller effect). Their model assumes discrete-state-continuum amplitudes independent of vibrational coordinates, which prohibits an indirect coupling of electronic states of different symmetries through the continuum. We extend this approach by considering the indirect coupling in a model for multiple discrete states and up to four vibrational degrees of freedom, which opens the possibility to treat the nonlocal dynamics of metastable states for a larger class of polyatomic molecular anions.

The $e + CO_2$ system is well suited to test the theoretical approach. First, the neutral molecule has an intriguing vibrational-level structure. Those $(\nu_1, \nu_2^{\ell}, \nu_3)$ harmonic levels that are nearly degenerate and have the same symmetry are strongly Fermi-coupled and distributed in polyads [14]. Second, there are many experimental data available [15]. Several aspects of the system are already well understood including the boomerang oscillations [16], threshold peaks in vibrational excitation [17], and sharing of excitation between members of the Fermi dyad [4,18]. On the other hand, some experimental data are still puzzling, especially those related to high vibrational excitation. Allan [19] reported a reappearance of structure in the spectra (with ~160 meV spacing) at nearly complete energy losses where Fermi-coupled polyads overlap and should form a dense structureless continuum (he termed it "spectroscopic order out of spectroscopic chaos"). Currell and Comer explained their data [14,20,21] as a result of excitation of very high bending modes and hypothesized that it is a signature of the quantum friction [22] in the CO_2^- nuclear motion. Up to this point, there have been no calculations that would provide an insight into the highly inelastic region. The Fermi coupling requires the inclusion of at least symmetric stretching and bending modes [23] and the most advanced treatment by McCurdy *et al.* [4] focused on excitation of low-lying vibrational states. In addition, theory has not addressed the sharing of excitation

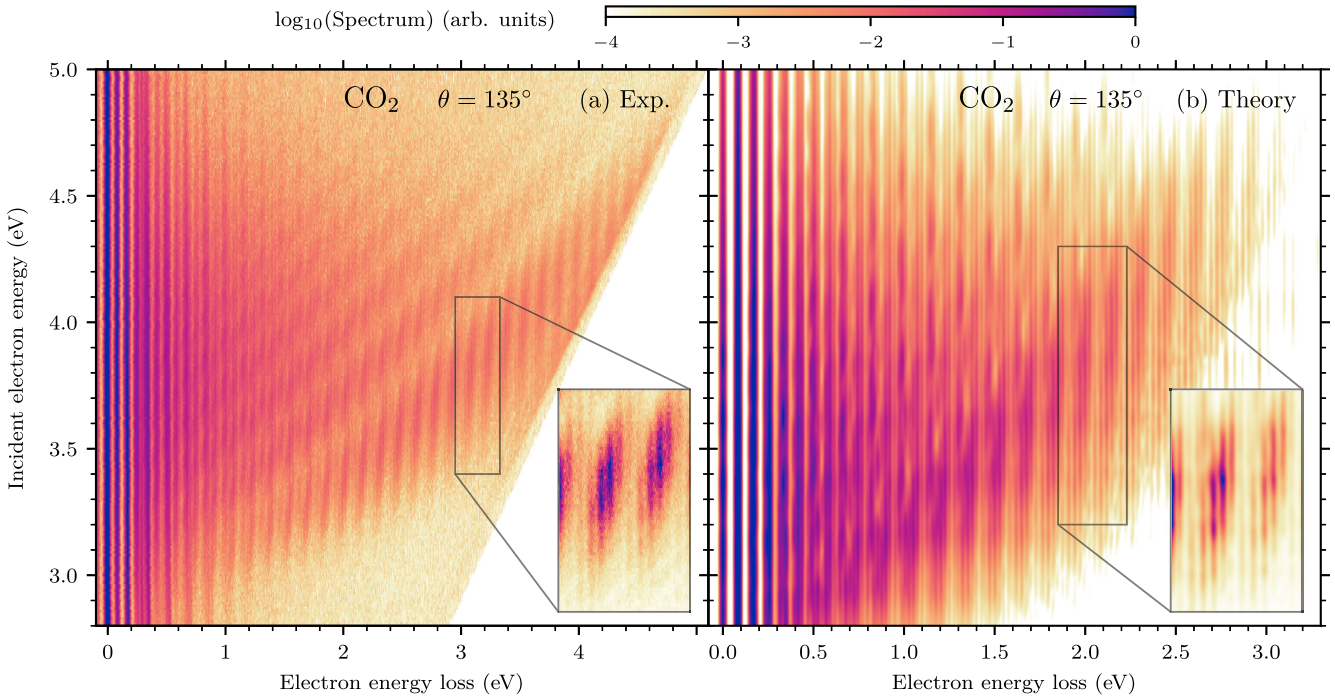

FIG. 1. (a) Experimental and (b) calculated 2D electron energy-loss spectra of CO_2 at a scattering angle of 135°. The main plots have the same logarithmic color scale shown at the top. The insets are in a linear scale from 0 to 1.

energies among nontotally symmetric vibrational states, such as odd quanta of bending or asymmetric stretching, which are clearly observed in experiments [15,24]. In this Letter, we interpret our new and also previously unexplained experimental observations of the $e + CO_2$ system based on nonlocal calculations of the nuclear dynamics, demonstrating the predictive power of our theoretical approach and at the same time the feasibility of the calculations.

We have experimentally probed the CO_2 vibrational excitation using the 2D electron energy-loss spectroscopy (EELS) [25,26] [Fig. 1(a)]. The incident electron energy (vertical axis) covers the region of the $^2\Pi_u$ resonance. The spectrum agrees well with previous reports, both classical 1D EELS studies [16,19,27–29] and early variants of 2D EELS [14,20,21]. However, the improved characteristics of the current experiment (energy resolution of 18 meV, sensitivity to electrons with residual energies down to 20 meV, high dynamic range) reveal new aspects. First, the "reappearing order" in 1D EELS spectra [19] corresponds to the lowest diagonal ray, which extends to complete energy losses. Second, the broad peaks in the high energy-loss region show a previously unreported fine structure [inset in Fig. 1(a)]. The spacing of this progression [empirically determined from 1D EELS spectrum, Fig. 2(a)] is ∼29 meV. Such a progression is surprising since first it is very different from the fundamental vibrational frequencies [30] (168 meV, 83 meV, and 297 meV for symmetric stretching, bending, and asymmetric stretching, respectively), and second, it appears in the region with a high vibrational level density. Therefore, there has to be some kind of selective mechanism. These results create an additional need for a proper multidimensional model of the vibrational excitation.

Our model is described in the companion paper [31]. Briefly, we consider three electronic states of CO_2^-: the $^2\Sigma_g^+$ virtual state and the $^2\Pi_u$ shape resonance, which splits due to the Renner-Teller effect into 2^2A_1 and $^2B_1$ states as the molecule bends [32]. The $^2\Sigma_g^+$ and $^2\Pi_u$ states were previously treated separately [4,18] and the topology of the PESs was unclear [33,34]. Sommerfeld *et al.* [34] argued that the virtual state and the 2^2A_1 Renner-Teller component mix upon bending, which couples all the three states together. We represent them by three diabatic discrete states $|d\rangle$ that are coupled directly through a potential matrix $V_{d_1 d_2} = \langle d_1|H_{\rm el}|d_2\rangle$, where $H_{\rm el}$ is the electronic Hamiltonian, and indirectly through the continuum by matrix elements $V^{\mu}_{d\epsilon} = \langle d|H_{\rm el}|\epsilon\mu\rangle$, which depend on electron energy ϵ. We consider the coupling to four electron partial waves $\mu \equiv (l, m)$ with $l = 0$, 1 for s, p waves, respectively. The coupling elements are functions of vibrational normal coordinates Q of all the modes but their form is restricted by the molecular symmetry [13,35]. To determine the model parameters we performed *ab initio* fixed-nuclei R-matrix calculations of eigenphase sums and PESs for thousands of molecular geometries using the UKRmol+ [36] suite of codes. The cuts of adiabatic PESs obtained within our model are shown in Fig. 3. All the

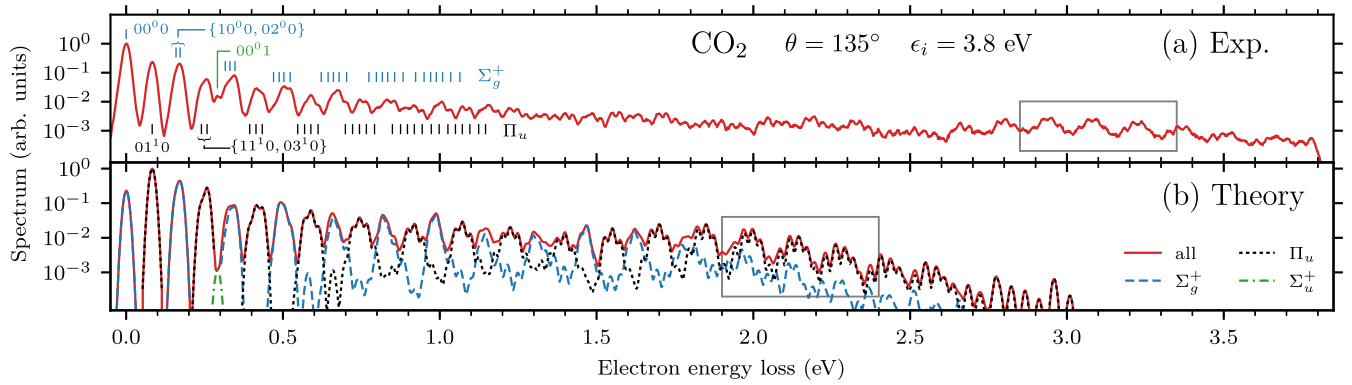

FIG. 2. (a) Experimental and (b) calculated 1D electron energy-loss spectra at a scattering angle of 135° and incident electron energy of 3.8 eV. We show the positions of the Σ_u^+ asymmetric stretching peak $(0, 0^0, 1)$ and vibrational states within Σ_g^+ polyads $(n, 2m^0, 0)$ and Π_u polyads $[n, (2m+1)^1, 0]$ for $n + m = 0, 1, \ldots, 6$. Panel (b) also shows calculated total contributions of Σ_g^+ and Π_u symmetries and the $(0, 0^0, 1)$ peak.

anionic states come close together and become bound as the molecule symmetrically stretches. The $^2B_1$ component is not much affected by the bending whereas the 2^2A_1 component rapidly moves to the threshold and its width significantly increases due to a strong coupling to the s wave. On top of that, this s-wave coupling gives rise to the local minimum in the 1^2A_1 potential but the minimum is connected with the $^2\Sigma_g^+$ virtual state while the 2^2A_1 state remains unbound.

The dynamics of CO_2^- for total energy E is described by the inhomogeneous Schrödinger equation $[E - T - V - F(E)]|\Psi\rangle = V_{\epsilon_i}^{\mu_i}|\nu_i\rangle$, where T is the kinetic energy of the vibrations, V is the potential matrix $V_{d_1 d_2}$, and the nonlocal level-shift operator matrix $F(E)$ is calculated by an integral transformation from $V_{d\epsilon}^{\mu}$ [3]. The scattering wave function $|\Psi\rangle$ has three vibrational components $\Psi_d(Q)$, which are expressed in a four-dimensional oscillator basis. This transforms the Schrödinger equation into a (large) system of linear equations, which we solved by the iterative conjugate orthogonal conjugate gradient (COCG) method [37] based on Krylov subspaces. Finally, the vibrational excitation cross sections are calculated from T-matrix elements $T_{\nu_f \mu_f \leftarrow \nu_i \mu_i} = \sum_d \langle \nu_f | V_{d\epsilon_f}^{\mu_f \dagger} | \Psi_d \rangle$, where ϵ_i and ϵ_f are the initial and final electron energies, μ_i and μ_f the incoming and outgoing electron partial waves, and ν_i and ν_f the initial and final vibrational states, respectively.

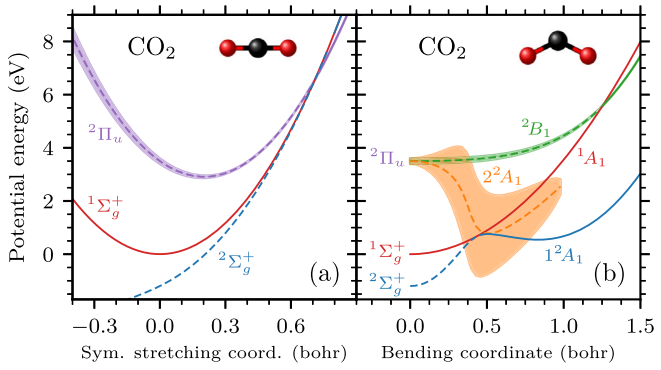

FIG. 3. Adiabatic potential energy curves of CO_2 (the ground state $^1\Sigma_g^+$) and CO_2^- ($^2\Sigma_g^+$, $^2\Pi_u$) within our model upon (a) symmetric stretching and (b) bending described by normal coordinates. The shaded areas represent the resonance widths.

Although anharmonic terms are included for the dynamics of the anion, the neutral molecule is only approximated by harmonic vibrations in order to keep the multidimensional calculations feasible. Thus, the dynamics does not include the Fermi resonance effect. Employing the anharmonic potential of Chedin [38], we calculated the expansion $|\nu_{\mathrm{FR}}\rangle = \sum_\nu c_\nu |\nu\rangle$ of the Fermi-coupled vibrational states $|\nu_{\mathrm{FR}}\rangle$ into harmonic states $|\nu\rangle$. By mixing the calculated harmonic T matrices using the coefficients c_ν, we partially incorporated this (crucial) effect.

To calculate the 2D spectrum shown in Fig. 1(b), we convoluted the cross sections with a Gaussian distribution to simulate the finite experimental resolution. First, we should explain a well-understood drawback of our model that influences the direct comparison with the experiment: the shrinking of the calculated energy-loss spectra towards lower energies. The used R-matrix model produces the vibrational frequencies about 30% larger than the experimental ones. Therefore, when we project the calculated population of the harmonic states after the collision to more precise Fermi-coupled levels (with lower energies), the spectrum shrinks towards lower energy losses. Apart from this quantitative difference, the model qualitatively reproduces the observed features and allows for their interpretation:

(i) Boomerang rays. Perhaps the most visually dominant features in the 2D spectrum are the diagonal rays. These are the boomerang oscillations [27] that originate from interference due to the back and forth motion of the nuclei in symmetric stretching [16]. They are known to be somewhat

weakened but not destroyed by the bending motion [23]. Calculated positions of boomerang peaks are also influenced by the above mentioned distortion and they do not directly correspond to the experimental data but the general character is reproduced.

(ii) Excitation of all modes. The dependence of the continuum coupling $V^{\mu}_{d\epsilon}$ on the vibrational coordinates allows excitation of nontotally symmetric vibrational states [39], which was not possible in previous calculations [4,18]. The excitation of the fundamental bending mode $(0, 1^1, 0)$ (marked in Fig. 2), which is of the Π_u symmetry, requires an electron that changes its angular momentum projection on the molecular axis. In our model, the electron has to come in as the p_x or p_y waves and leave as the s wave or vice versa, which is controlled by $V^{\mu}_{d\epsilon}$ proportional to the bending coordinate. Similarly, the excitation of the asymmetric stretching $(0, 0^0, 1)$ (also marked in Fig. 2) of the Σ^+_u symmetry requires a change from p_z wave to s or from s to p_z.

(iii) "Spectroscopic order out of spectroscopic chaos." Allan [19] pointed out that the experimental 1D EELS spectrum [such as the one in Fig. 2(a)] shows a very regular character at low energy losses (here up to some 1.3 eV), then the spectrum is seemingly structureless (1.3–2.5 eV), and above 2.5 eV a new regular peak progression appears (the resolution in [19] was insufficient to resolve the fine structure). Our model explains this behavior by selectivity of different polyads [Fig. 2(b)]. Overall, the dominantly populated vibrational states $|\nu_{\mathrm{FR}}\rangle$ are even polyads composed of harmonic basis states $\nu = (n, 2m^0, 0)$ of the Σ^+_g symmetry and odd polyads composed of $[n, (2m+1)^1, 0]$ of the Π_u symmetry, where $n + m = N =$ constant identifies individual polyads. For example, states within the Π_u polyad with $N = 12$ are linear combinations of $\nu = (12, 1^1, 0), (11, 3^1, 0), \ldots, (0, 25^1, 0)$ and the corresponding amplitudes c_ν are typically non-negligible for all the states. At first, Σ^+_g and Π_u peaks are well distinguishable since the Π_u peaks are shifted by one bending quantum. At intermediate energy losses, energy ranges of the polyads start to overlap and create seemingly chaotic patterns because of the similar magnitude of the excitation. In the high energy-loss region, the Π_u excitation dominates and the order is partially restored. This behavior is related to a change of the electron angular momentum from p to s discussed above. The incoming electron is dominantly of the p-wave character due to the existence of the 3.8 eV resonance. At high electron losses, the outgoing p-wave contribution with a small residual energy is suppressed due to the threshold law of Wigner [40]. The electron thus preferably leaves as an s wave forcing the change of angular momentum in the vibrational state leading dominantly to Π_u states.

(iv) Fine structure at high energy losses. Figure 4 depicts a detail of the 1D EELS spectra in the region dominated by the Π_u contribution as indicated by frames in Fig. 2.

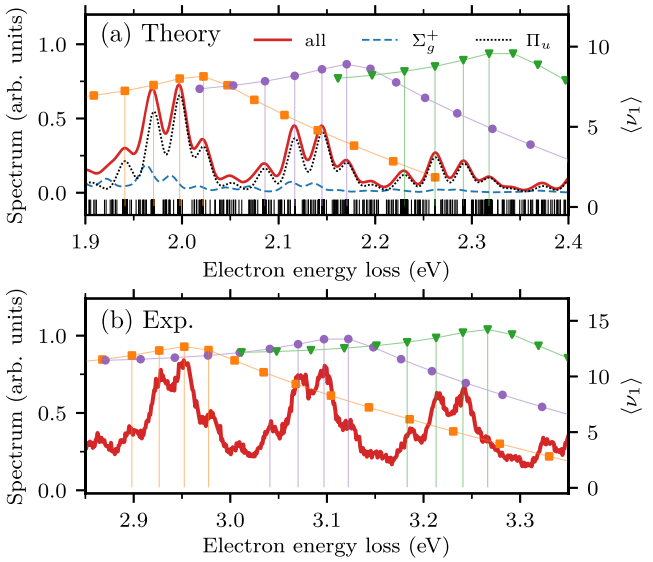

FIG. 4. (a) Theoretical and (b) experimental fine structures at high energy losses. The symbols represent the mean value of number of symmetric stretching quanta $\langle\nu_1\rangle$, see the text, for members of Π_u polyads $[n, (2m+1)^1, 0]$ with $n + m = 12$, 13, 14 for the theoretical spectrum and $n + m = 18$, 19, 20 for the experimental result. Panel (a) also shows contributions of Σ^+_g and Π_u vibrational states and the vertical lines at the bottom indicate energies of all relevant vibrational states included in our model.

From the calculation we know which individual state is responsible for each peak in the theoretical spectrum. To understand it more, we characterize the Fermi-coupled states $|\nu_{\mathrm{FR}}\rangle$ by the mean value of number of symmetric stretching quanta $\langle\nu_1\rangle = \sum_\nu \nu_1 |c_\nu|^2$. In Fig. 4(a), the horizontal positions of the symbols show the theoretical energies of the states within the Π_u polyads with $N = 12$, 13, 14 and vertical positions represent the $\langle\nu_1\rangle$ values. Even though the polyads significantly overlap, only one polyad is responsible for each broad peak and the fine structure is given by the excitation of consecutive states somewhat below the maximum of $\langle\nu_1\rangle$. These fairly linear states are dominantly localized in the vibrational space along the symmetric stretching axis. Highly bent states, which are located at both ends of the polyads, are not significantly populated because the rapid broadening of the 2^2A_1 state causes a fast decay of the anion in highly bent nuclear configurations, see Fig. 3(b). To verify this mechanism, we plot the same quantity $\langle\nu_1\rangle$ for Π_u polyads with $N = 18$, 19, 20 to the experimental spectrum in Fig. 4(b). We found out that the positions of the predicted peaks follow very well the experimental peaks not only in the showed energy-loss interval but also in the spectra for other incident electron energies.

(v) Alternating excitation pattern in diagonal rays. Currell and Comer [14,21] observed two types of excitation, which they labeled by A and B, alternating in the diagonal rays of the 2D spectrum for intermediate energy

losses at a small scattering angle. We also observe the same patterns in our spectra at 135°. They correctly assigned the type A excitation to excitation of linear vibrational states of the Σ_g^+ polyads $(n, 2m^0, 0)$. However, they argued that the type B excitation is caused by decay to highly bent states of the same polyads via the quantum friction effect [22]. Our calculations show that this is not the case and that fairly linear states of the Π_u symmetry are responsible for the type B excitation.

In conclusion, the present nonlocal model qualitatively explains the observed features of the $e + CO_2$ system. The high energy-loss region is primarily influenced by the change of the incoming resonant p wave into the outgoing s wave, which leads to excitation of vibrational states of the Π_u symmetry. The model also singles out the states that are responsible for the emergence of the fine structure from the pseudocontinuum of available states. The theoretical approach, presented here on the example of the CO_2 molecule, can provide the explanation of the behavior of other polyatomic systems as well since the change of the electron symmetry and the consequential excitation of nontotally symmetric vibrational modes appear to be an important phenomenon [39,41–46].

We thank Michael Allan for inspiring discussions. This work was supported by the Czech Science Foundation Projects No. 19-20524S (M. Č., K. H., J. D.), No. 20-11460S (J. F.), and No. 21-12598S (R. Č.) and by the Charles University Grant Agency, Project No. 552120 (J. D., M. Č.).

*Corresponding author.
juraj.fedor@jh-inst.cas.cz
†Corresponding author.
martin.cizek@mff.cuni.cz

[1] H. Hotop, M.-W. Ruf, M. Allan, and I. Fabrikant, Adv. At. Mol. Opt. Phys. **49**, 85 (2003).
[2] I. I. Fabrikant, S. Eden, N. J. Mason, and J. Fedor, Adv. At. Mol. Opt. Phys. **66**, 545 (2017).
[3] W. Domcke, Phys. Rep. **208**, 97 (1991).
[4] C. W. McCurdy, W. A. Isaacs, H.-D. Meyer, and T. N. Rescigno, Phys. Rev. A **67**, 042708 (2003).
[5] D. J. Haxton, T. N. Rescigno, and C. W. McCurdy, Phys. Rev. A **75**, 012711 (2007).
[6] S. T. Chourou and A. E. Orel, Phys. Rev. A **80**, 032709 (2009).
[7] H. B. Ambalampitiya and I. I. Fabrikant, Phys. Rev. A **102**, 022802 (2020).
[8] S. Feuerbacher, T. Sommerfeld, and L. S. Cederbaum, J. Chem. Phys. **120**, 3201 (2004).
[9] S. Feuerbacher and L. S. Cederbaum, J. Chem. Phys. **121**, 5 (2004).
[10] D. J. Haxton, T. N. Rescigno, and C. W. McCurdy, Phys. Rev. A **72**, 022705 (2005).
[11] D. J. Haxton, C. W. McCurdy, and T. N. Rescigno, Phys. Rev. A **75**, 012710 (2007).
[12] H. Köppel, W. Domcke, and L. S. Cederbaum, Multimode Molecular Dynamics Beyond the Born-Oppenheimer Approximation, in *Advances in Chemical Physics* (John Wiley & Sons, Ltd, New York, 1984), pp. 59–246.
[13] H. Estrada, L. S. Cederbaum, and W. Domcke, J. Chem. Phys. **84**, 152 (1986).
[14] F. Currell, J. Phys. B **29**, 3855 (1996).
[15] M. Allan, J. Phys. B **35**, L387 (2002).
[16] I. Čadež, F. Gresteau, M. Tronc, and R. I. Hall, J. Phys. B **10**, 3821 (1977).
[17] H. Estrada and W. Domcke, J. Phys. B **18**, 4469 (1985).
[18] W. Vanroose, Z. Zhang, C. W. McCurdy, and T. N. Rescigno, Phys. Rev. Lett. **92**, 053201 (2004).
[19] M. Allan, J. Electron Spectrosc. Relat. Phenom. **48**, 219 (1989).
[20] F. Currell and J. Comer, J. Phys. B **26**, 2463 (1993).
[21] F. Currell and J. Comer, Phys. Rev. Lett. **74**, 1319 (1995).
[22] W. Domcke and H. Estrada, J. Phys. B **21**, L205 (1988).
[23] T. N. Rescigno, W. A. Isaacs, A. E. Orel, H.-D. Meyer, and C. W. McCurdy, Phys. Rev. A **65**, 032716 (2002).
[24] M. Allan, Phys. Rev. Lett. **87**, 033201 (2001).
[25] K. Regeta and M. Allan, Phys. Rev. Lett. **110**, 203201 (2013).
[26] C. S. Anstöter, G. Mensa-Bonsu, P. Nag, M. Ranković, T. P., R. Kumar, A. N. Boichenko, A. V. Bochenkova, J. Fedor, and J. R. R. Verlet, Phys. Rev. Lett. **124**, 203401 (2020).
[27] M. J. W. Boness and G. J. Schulz, Phys. Rev. A **9**, 1969 (1974).
[28] S. Cvejanovic, J. Jureta, and D. Cvejanovic, J. Phys. B **18**, 2541 (1985).
[29] D. F. Register, H. Nishimura, and S. Trajmar, J. Phys. B **13**, 1651 (1980).
[30] D. M. Dennison, Rev. Mod. Phys. **12**, 175 (1940).
[31] J. Dvořák, K. Houfek, and M. Čížek, companion paper, Phys. Rev. A **105**, 062821 (2022).
[32] L. A. Morgan, Phys. Rev. Lett. **80**, 1873 (1998).
[33] W. Vanroose, C. W. McCurdy, and T. N. Rescigno, Phys. Rev. A **66**, 032720 (2002).
[34] T. Sommerfeld, H.-D. Meyer, and L. S. Cederbaum, Phys. Chem. Chem. Phys. **6**, 42 (2004).
[35] H. Köppel, W. Domcke, and L. S. Cederbaum, J. Chem. Phys. **74**, 2945 (1981).
[36] Z. Mašín, J. Benda, J. D. Gorfinkiel, A. G. Harvey, and J. Tennyson, Comput. Phys. Commun. **249**, 107092 (2020).
[37] H. van der Vorst and J. Melissen, IEEE Trans. Magn. **26**, 706 (1990).
[38] A. Chedin, J. Mol. Spectrosc. **76**, 430 (1979).
[39] G. A. Gallup, J. Chem. Phys. **99**, 827 (1993).
[40] E. P. Wigner, Phys. Rev. **73**, 1002 (1948).
[41] S. F. Wong and G. J. Schulz, Phys. Rev. Lett. **35**, 1429 (1975).
[42] G. A. Gallup, Phys. Rev. A **34**, 2746 (1986).
[43] R. Čurík, I. Paidarová, M. Allan, and P. Čársky, J. Phys. Chem. A **118**, 9734 (2014).
[44] R. Čurík, P. Čársky, and M. Allan, J. Chem. Phys. **142**, 144312 (2015).
[45] C. H. Yuen, N. Douguet, S. Fonseca dos Santos, A. E. Orel, and V. Kokoouline, Phys. Rev. A **99**, 032701 (2019).
[46] P. Nag, R. Čurík, M. Tarana, M. Polášek, M. Ehara, T. Sommerfeld, and J. Fedor, Phys. Chem. Chem. Phys. **22**, 23141 (2020).